

## Measurements of helium adsorption on natural clinoptilolite at temperatures from (123.15 to 423.15) K and pressures up to 35 MPa

Arash Arami-Niya<sup>a, b</sup>, Thomas E. Rufford<sup>a</sup>, Gerrit Drespe<sup>c</sup>, Saif Al Ghafri<sup>b</sup>, Fuyu Jiao<sup>b</sup>, Eric F. May<sup>b, \*</sup>

*a. School of Chemical Engineering, The University of Queensland, St Lucia 4072 Australia*

*b. Fluid Science & Resources Division, Department of Chemical Engineering, The University of Western Australia, Crawley, WA 6009, Australia*

*c. Thermodynamics, Ruhr-University Bochum, Universitätsstraße 150, 44801 Bochum, Germany*

### Abstract

Helium (He) is an increasingly valuable gas that is relatively difficult to recover: most of the global helium supply is produced through the application of deep cryogenic separation processes to the overheads from a nitrogen rejection unit in an LNG plant. Pressure swing adsorption (PSA) offers an alternative low-cost process for recovering He from natural gas, particularly if a helium selective adsorbent with sufficient capacity could be identified. However, the accurate measurement of the helium equilibrium capacity on narrow pore adsorbents is particularly challenging. Here, the uptake of helium on a natural clinoptilolite-rich Escott zeolite was measured with a volumetric adsorption apparatus at temperatures from 123.15 – 423.15 K and pressures up to 5 MPa, and with a gravimetric adsorption apparatus at temperatures in the range 243.15 – 423.15 K and pressures up to 35 MPa. We used these two experimental data sets to determine the specific inaccessible solid volume ( $v_s$ ) and true void volume of the Escott zeolite by eliminating the common assumption of zero helium uptake. Instead, the data analysis workflow established by Sircar<sup>1</sup> and by Gumma and Talu<sup>2</sup> was applied to the adsorption isotherms measured using the gravimetric apparatus. This led to a specific inaccessible solid volume for the Escott zeolite of  $0.462 \text{ cm}^3 \cdot \text{g}^{-1}$ , with a maximum helium adsorption capacity of  $0.9 \text{ mmol} \cdot \text{g}^{-1}$  measured at 253.15 K and 35 MPa. The **isosteric** heat of adsorption for helium on the Escott zeolite was estimated to be  $3.05 \text{ kJ} \cdot \text{mol}^{-1}$ . The uptake of  $\text{N}_2$  on the Escott zeolite was also measured; these data were used together with the helium measurements to estimate conditions at which an equilibrium selectivity of 3 for He over  $\text{N}_2$  might be achieved in an equimolar He +  $\text{N}_2$  mixture.

## Nomenclature

$H$	Henry's constant, (mmol.(g.kPa) <sup>-1</sup> )
$H_0$	Entropy of adsorption, (mmol.(g.kPa) <sup>-1</sup> )
$H_1$	Isotheric heat of adsorption, (kJ.mol <sup>-1</sup> )
$m_{ads}$	Adsorbed phase weight, (g)
$m_b$	True weight of sample basket, (basket and hook), (g)
$m_s$	True weight of solid adsorbent, (g)
$m_{bal}$	corrected mass recorded by balance at measuring point 1, (g).
$m_t^{Calc}$	Calculated total weight, (g)
$m_t^{Meas}$	Measured total weight, (g)
$m_w$	Molecular weight of adsorbate (helium), (g)
$n_{ads}$	Number of moles in the adsorption cell (mmol)
$n_L$	Number of moles in the loading cell (mmol)
$n_{Ads}$	Number of moles adsorbed (mmol)
$P$	Pressure, (MPa)
$Q_a$	Amount of helium adsorbed per unit mass of the adsorbent, (mmol.g <sup>-1</sup> )
$R$	Molar gas constant, (kJ.(K.mol) <sup>-1</sup> )
$V_{ads}$	Volume of adsorbed phase, (cm <sup>3</sup> )
$V_A$	Volume of adsorption cell, (cm <sup>3</sup> )
$V_b$	Sample basket (basket and hook) volume, (cm <sup>3</sup> )
$V_L$	Volume of loading cell, (cm <sup>3</sup> )
$V_s$	Impenetrable solid volume, (cm <sup>3</sup> )
$v_s$	Specific inaccessible solid volume, (cm <sup>3</sup> /g <sup>-1</sup> )
$V_t$	Total volume, (cm <sup>3</sup> )
$\rho_g$	Fluid density, (g/cm <sup>-3</sup> )
$\Delta m$	Raw mass change, (g)

## 1 Introduction

In common gas adsorption measurement techniques, helium is typically used for free space determination under the assumption that helium adsorption is negligible at ambient temperature and pressure<sup>3-4</sup>. Although sorption of helium is generally quite small at ambient condition, in some materials, such as particular polymers<sup>5</sup> or small pore adsorbents<sup>6-7</sup>, helium interaction with the solid surface is not negligible. In fact, many studies of microporous materials show sufficient affinity for helium<sup>1, 5-6, 8-9</sup> to cause an appreciable violation of the zero helium adsorption assumption central to the determination of the solid's true volume and/or the dead volume surrounding the sample. Meggs et al.<sup>6</sup> showed that the apparent density of microporous activated carbons determined by the use of helium and application of the ideal gas law to pressure/volume data acquired at room temperature with conventional volumetric adsorption apparatus can produce deviations of up to 14 % from the sample's actual density. Malbrunot et al.<sup>3</sup> studied helium adsorption on different adsorbents including zeolite 3A, 4A, 5A, and 13X, activated carbon, and silica gel over a large temperature range of 273.15 to 673.15 K. Through comparisons with results obtained for non-porous graphitized carbon black, they concluded that the apparent adsorbent densities determined from room temperature measurements using helium could be erroneous by up to 36% due to a non-negligible adsorption effects.

Measuring the helium adsorption capacity of materials is challenging<sup>5</sup>, but it is important for correct dilatometric analysis of porous solids. Different approaches have been reported in the literature to determine simultaneously a material's solid volume and measure its helium adsorption capacity. One method involves the use of helium at high temperature, for instance, at the regeneration temperature of the adsorbent<sup>3, 6</sup>. This method was used by Suzuki et al. to measure helium adsorption on several zeolites over the temperature range of 77 to 673 K. They compared the increase in apparent dead space between the cell containing the adsorbent and a reference cell containing several glass rods on the assumption of negligible helium adsorption at 673 K<sup>8</sup>. Maggs et al. analyzed the effect of temperature on the apparent dead-space of a conventional volumetric apparatus to determine the extent of helium adsorption by assuming that the adsorption isotherms were linear<sup>6</sup>.

The assumption that helium is non-adsorbing at a certain condition is not essential for the purpose of decoupling solid density and helium capacity determinations. Gumma and Talu<sup>2</sup> proposed a self-consistent method to determine the Gibbs dividing surface for a material (which effectively sets its volume) and its helium adsorption capacity. We applied Gumma and Talu's method in our previous study<sup>10</sup> to measure the true density of natural clinoptilolite (Escott

zeolite) and its helium adsorption capacity over the range 298 – 343 K and at pressures up to 3.5 MPa using a gravimetric apparatus. However, that instrument's limitations prevented the extension of the measurements to wider ranges of temperature and pressure. In this study, we used two different apparatus based on the volumetric and gravimetric techniques to extend the measurement of helium adsorption on the natural zeolite to temperatures from (123.15 to 423.15) K and pressures to 35 MPa. These wide-ranges of temperature and pressure makes this study one of the most extensive investigations of helium adsorption on a narrow pore adsorbent. The adsorption of helium was most evident at low temperatures and high pressures, and the data acquired allow quantification of the effect of helium adsorption on the measurement of the solid's true volume. We also measured the N<sub>2</sub> adsorption capacity of the natural clinoptilolite at temperatures of 303-323 K and pressures up to 4.5 MPa and then analyzed the IAST calculations of equilibrium selectivity for He over N<sub>2</sub>. The results of this study provide the preliminary information necessary to design an adsorption-based, helium-selective process using small pore adsorbents that reject the heavier components (mostly N<sub>2</sub> and/or CH<sub>4</sub>) from the overhead stream of a nitrogen rejection unit in a LNG plant.

## 2 Experimental

Natural clinoptilolite-rich Escott zeolite<sup>11</sup> from the Werris Creek deposit (New South Wales, Australia) was provided by Zeolite Australia Pty Limited. The zeolite was used as-received, chipped in 1 - 2.2 mm size granules. The supplier's technical data sheet indicates that this natural zeolite is rich in clinoptilolite, which is a narrow-pore zeolite classified in the heulandite (HEU) group and has a typical unit cell of Na<sub>6</sub>[(Al<sub>2</sub>O<sub>3</sub>)<sub>8</sub>(SiO<sub>2</sub>)<sub>28</sub>].24H<sub>2</sub>O. Previously<sup>10</sup>, we confirmed the presence of clinoptilolite in the Escott sample by powder X-ray diffraction and MAS NMR spectra, and reported other pore textural properties of the Escott. The purity of helium and nitrogen used in this work, as stated by the supplier Coregas Australia, was Grade 5 (99.999 mol%).

### 2.1 Determination of solid true volume and equilibrium helium adsorption measurements

#### 2.1.1 High-pressure volumetric adsorption apparatus

A schematic of the custom built volumetric adsorption apparatus is shown in **Figure 1**. The construction and operation of this apparatus is described in detail elsewhere<sup>12-14</sup>. Here, we provide a brief description of the key features of this apparatus, the procedures followed to calibrate its internal volumes, and the experimental workflow used to measure helium adsorption.

The volumes of the loading cell ( $V_L$ ) and the adsorption cell ( $V_A$ , before loading the adsorbent sample) were gravimetrically determined in the range of experimental temperatures using argon as a reference gas. The mass of argon required to raise the pressure in the loading cell to a value around 3.5 MPa was determined by weighing a small sample cylinder (about 1 kg total mass) before and after the transfer of gas to the loading cell. The change in mass (around 13 g) was equated to the product of the gas density and volume of the loading cell. The density of the argon at the temperature and pressure measured in the loading cell was determined using the reference equation of state (EOS) of Tegeler et al.<sup>15</sup> as implemented in the NIST software package REFPROP 9.1<sup>16</sup>. The volume calibration was repeated twice with argon, and then the calculated  $V_L = 771.14 \pm 0.76 \text{ cm}^3$  at 303.15 K was validated to within the estimated uncertainty using another gravimetric measurement with nitrogen. Before loading the adsorbent, the same gravimetric procedure was used to calibrate the adsorption cell volume across the range of measurement temperatures ( $276.07 \pm 0.3 \text{ cm}^3$  at 343.15 K and  $269.68 \pm 0.4 \text{ cm}^3$  at 143.15 K) which is consistent with thermal expansion of stainless steel. Watson et al.<sup>12</sup> showed that the dilation of the adsorption and loading cells with pressure contributes a negligible uncertainty to the volume of either cell.

The loading cell was immersed in a water bath held at a constant temperature of 298 K. The adsorption cell was housed inside a three-stage thermostat, where temperatures were controlled with proportional integral control loops that adjusted the electrical power supplied to thermfoil-type heaters located on the exterior of the adsorption cell and copper can. The temperature of the adsorption cell was measured with six  $100 \Omega$  platinum resistance thermometers (PRT), which were calibrated to ITS-90 over the range 77 K to 303 K with an estimated uncertainty of 0.05 K. The pressure in the adsorption cell was measured using a quartz crystal transducer with a full scale of 7 MPa and an estimated uncertainty over this range of  $4 \times 10^{-4}$  MPa.

Prior to the adsorption measurements, the Escott zeolite was degassed in a separate regeneration cell under vacuum ( $1 \times 10^{-3}$  Torr) at 623 K for 24 hours. The regeneration cell was backfilled with  $\text{N}_2$  to minimize air ingress during transfer of the adsorbent to the adsorption cell of the volumetric apparatus. The mass of degassed Escott loaded to the stainless steel sample basket to be placed in the adsorption cell was  $m_{\text{ads}} = 44.151 \pm 0.001 \text{ g}$ . The loaded sample was then degassed in situ at 353 K under a vacuum of  $1 \times 10^{-3}$  Torr for another 24 hours. The in situ regeneration of the sample was repeated after the measurements of each isotherm.

In a typical measurement, the loading cell was filled with the adsorbate gas (helium), and the cell allowed to reach thermal stability by waiting for at least one hour. Then the initial number of moles of gas in the loading cell ( $n_L^i$ ) was calculated from the calibrated volume of the loading cell ( $V_L$ ) and the gas density ( $\rho_g(T, P)_L^i$ ) at the loading cell temperature ( $T_L$ ) and pressure ( $P_L$ ) using the reference equation of state for helium by Ortiz-Vega et al. as implemented in the NIST software package REFPROP 9.1<sup>16</sup>. Gas was delivered to the adsorption cell by opening valve V2 shown in **Figure 1**, and the system allowed to stabilize again before recording the equilibrium temperature and pressure of the loading cell to calculate the final gas density ( $\rho_g(T, P)_L^f$ ) and moles of gas remaining in the loading cell  $n_L^f$ . From this procedure, the number of moles of gas transferred to the adsorption cell ( $\Delta n_L$ ) can be determined with Equation 1:

$$\Delta n_L = n_L^i - n_L^f = [\rho_g(T, P)_L^i - \rho_g(T, P)_L^f] \times V_L(T) \quad (1)$$

After the transfer of gas to the adsorption cell, the equilibrium adsorption cell temperature and pressure were used to calculate the gas density in the adsorption cell ( $\rho_g(T, P)_A$ ). The number of moles of gas remaining in the void space of the adsorption cell ( $n_A$ ) can be computed using the calibrated volume of the empty adsorption cell ( $V_A$ ) and, if known, the solid volume of the adsorbent ( $V_s$ ), as in Equation 2:

$$n_A = \rho_g(T, P)_A \times [V_A(T_A) - V_s(T_A)] \quad (2)$$

Finally, the number of moles adsorbed ( $n_{Ads}$ ) are calculated by a mole balance on the adsorption cell:

$$n_{Ads} = \Delta n_L - n_A \quad (3)$$

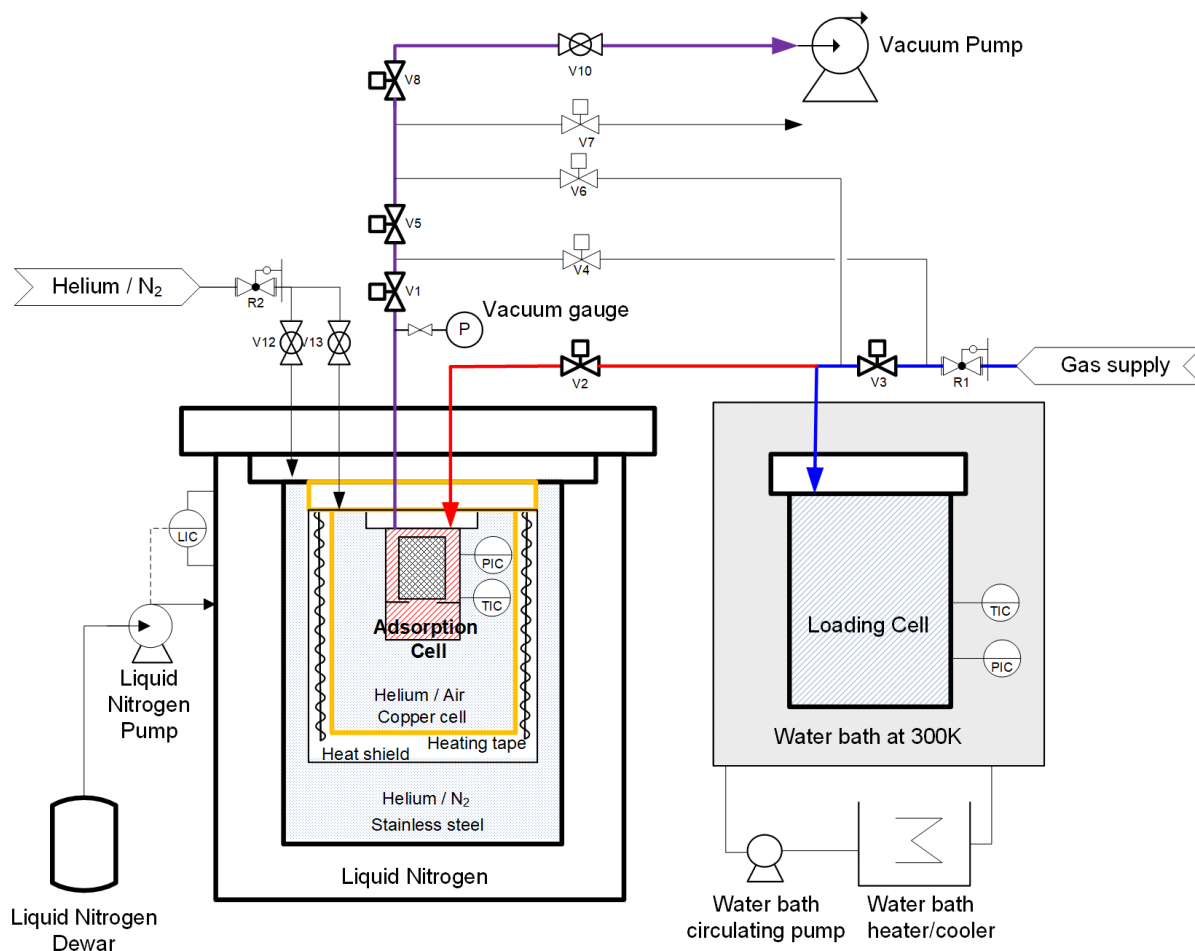


**Figure 1** A schematic of the custom built high pressure volumetric apparatus.

### 2.1.2 Gravimetric adsorption apparatus

The gravimetric helium adsorption measurements were performed at temperatures in the range (253.15 - 423.15) K and pressures up to 35 MPa on an IsoSORP commercial magnetic-suspension balance (Rubotherm, Bochum, Germany). The Rubotherm microbalance was a Mettler WXS series with a weighing range of 20 g and resolution of 1  $\mu\text{g}$ <sup>17</sup>. The resolution of this microbalance is 10 times better than that of the Belsorp instrument (10  $\mu\text{g}$ ) used in our previous studies of helium adsorption on Escott zeolite (Arami-Niya, et al.<sup>10</sup>), and the maximum operating pressure is also 10 times larger.

The schematic of the IsoSorp apparatus in *Figure 2* shows how the microbalance is capable of measuring the combined weight of the sinker and the adsorption basket by means of a magnetic-suspension coupling. The key components of this coupling are the electromagnet

connected to the microbalance outside the pressure vessel and the suspended permanent magnet attached to the sinker + basket inside the vessel. The stable suspension of the permanent magnet inside the adsorption cell was realized by a PID control circuit connected to a position transducer. The position transducer consists of a fixed sensor coil on the body of the cell and a suspended sensor core, which is attached to the coupling rod between the permanent magnet and the sinker + basket. The magnetic suspension microbalance records two stable suspension positions during a single step of an adsorption measurement. First a measurement at the *zero point* (ZP) is acquired to correct for any drift in the balance between data points in an isotherm measurement. Next, measurement point 1 (MP1) is selected where the weight of the basket will be measured. A second measurement point (MP2) can be selected, where a non-porous sinker of known volume is weighed to determine the gas density via a buoyancy correction. This was unnecessary in the present work because the equation of state for helium allowed the gas density to be determined from the measured pressure and temperature to within 0.05 %<sup>16</sup>; thus the apparatus was never set to MP2 in this work.

The temperature inside the gravimetric adsorption cell was measured with a 100  $\Omega$  PRT, which was calibrated on ITS-90 by comparison to a reference thermometry chain with a standard uncertainty of 0.03 K. The temperature of the cell was controlled by the circulation of mineral oil and ethanol at temperatures above and below 298 K, respectively, into a metallic jacket surrounding the adsorption cell. The jacket was fully insulated to avoid temperature fluctuations in the system due to the changes in ambient temperature. The pressure in the adsorption cell was measured using a vibrating quartz-crystal pressure transducer, (9000-6K-101, Paroscientific, Redmond, WA, USA) with a full scale of 40 MPa and an uncertainty within 0.01 % of this maximum pressure.



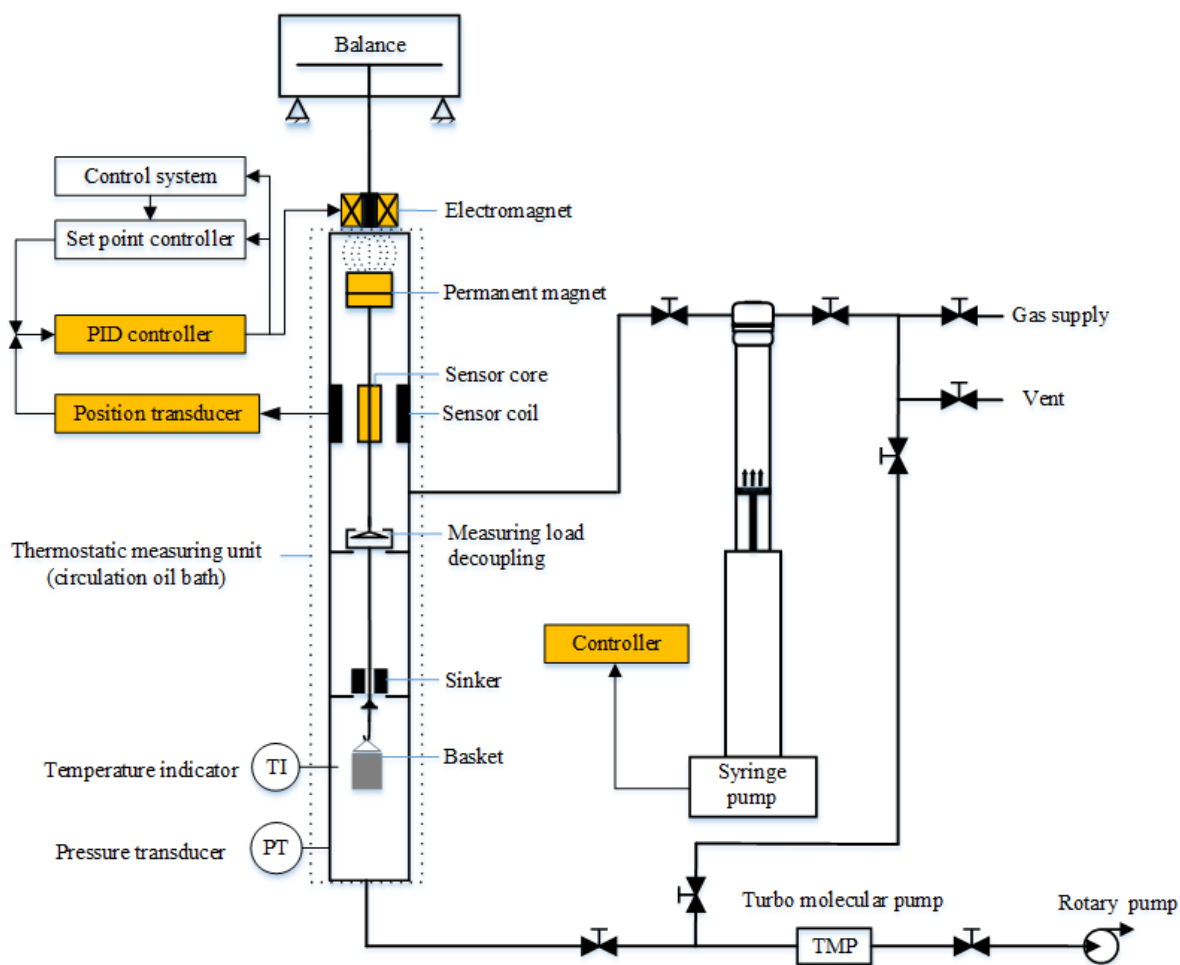


Figure 2 Schematic of the IsoSorp gravimetric adsorption apparatus.

Prior to the gravimetric adsorption measurements, 3.75 g of Escott was degassed at 623.15 K in an oven (heating rate of  $1 \text{ K}\cdot\text{min}^{-1}$ ) under a vacuum of  $1 \times 10^{-3}$  Torr for 24 hours. Then, the sample was transferred to the Rubotherm apparatus and degassed in-situ at 433.15 K under an ultimate vacuum of  $1 \times 10^{-5}$  Torr, or lower, for 12 hours to remove any contaminants adsorbed from the air during transfer. After degassing, the mass of the solid adsorbent ( $m_s$ ) was recorded under the vacuum condition.

After the in-situ degassing, the Rubotherm apparatus temperature was set to the desired temperature and the cell was filled with helium injected from an Isco syringe pump (260D High-Pressure Pump, Teledyne Isco, USA) to the desired measurement pressure. The system was then left equilibrate, which was assumed to have occurred when the mass recorded by the balance was stable with a variation less than  $20 \mu\text{g}$  over a 10 minute period. The mean values for temperature, pressure and mass recorded over a subsequent period of at least 30 minutes

after reaching equilibrium are reported in Table 1S.

The absolute mass of adsorbed gas ( $m_{ads}$ ) was determined by first measuring the corrected mass recorded by the balance at measuring point 1 ( $m_{bal}$ ):

$$m_{bal} = MP1 - ZP \quad (4)$$

This value of  $m_{bal}$  includes the mass of the sample basket and balance hook ( $m_b$ ), the mass of the solid adsorbent ( $m_s$ ), the mass of the adsorbed phase ( $m_{ads}$ ), and a contribution (reduction) to the apparent mass due to the buoyancy effect of the surrounding fluid (i.e., Archimedes principle). The force balance is shown in Equation 5:

$$m_{bal} = m_b + m_s + m_{ads} - \left[ (V_b + V_s + V_{ads}) \rho_g \right] \quad (5)$$

The last term in Equation 5 describes the effect of buoyancy of the gas density ( $\rho_g$ ) applied to the volume of the sample basket and balance hook ( $V_b$ ), the volume of the solid adsorbent ( $V_s$ ) and the volume of the adsorbed phase ( $V_{ads}$ ).

The (apparent) mass of the sample basket and balance hook ( $m_b \approx 5.09$  g) was determined by a measurement under high vacuum at different experimental temperatures. The balance housing was filled with (static) air for measurements at  $T > 273.15$  K. At lower temperatures ( $T < 273.15$  K), the housing was flushed with a small continuous flow of ambient pressure argon to prevent water vapor from the air condensing on the electromagnet of the suspension coupling inside the central tube connecting the balance housing with the coupling housing. As explained by Karimi et al.<sup>17</sup> the density of argon was used to evaluate the buoyancy correction to the balance's internal stainless steel calibration masses at these temperatures (rather than the density of air, which was used at  $T > 273.15$  K). The thermally-induced changes in the magnetic susceptibility of the pressure vessel, which influences the strength of the magnetic coupling was accounted for through a volume calibration of the sample basket and balance hook. The corresponding volume of the sample basket and hook ( $V_b \approx 0.65$  ml at 273.15 K) was determined at various experimental temperatures and pressures using argon as a calibration gas using the method explained by Karimi et al.;<sup>17</sup> the results are presented in Table 3S. The volume of adsorbed phase ( $V_{ads}$ ) was assumed to be negligible compared to the basket and solid volume ( $V_b + V_s$ ) because the absolute volume of helium adsorbed is very small. Therefore, the only remaining unknown parameter in Equation 5 required to calculate  $m_{ads}$  is the solid adsorbent volume,  $V_s$ .

### 2.1.3 Determination of solid true volume

In a conventional measurement with a volumetric apparatus, the sample volume  $V_s$  is typically determined by a helium dilatometry experiments performed at low pressure and by assuming that helium adsorption at this condition is negligible. In section 3.1 of this manuscript we explore the validity of that assumption by calculating the specific volume of the adsorbent ( $v_s = V_s / m_s$ ) at each measurement temperature from (123 – 423.15) K subject to the assumption  $n_{Ads} = 0$  at each condition.

In section 3.2 we apply the approaches Sircar<sup>1</sup> and Gumma and Talu<sup>2</sup> to deduce the true solid specific volume. Proposed initially by Sircar<sup>1</sup> and then developed by Gumma and Talu<sup>2</sup>, the method considers helium as an adsorbing gas at all experimental temperatures. It is possible to calculate the solid specific volume ( $v_s$ ) using Equation 5, if the mass of the adsorbed phase ( $m_{ads}$ ) could be determined. To do this, Henry's law is applied to determine the surface excess of helium as function of experimental temperature and pressure ( $n_{ads} = HP$ )<sup>18</sup>; use of Henry's law is justified given the small interaction of helium with the solid surface, particularly at low to moderate pressures where the adsorption isotherm is linear. The mass of the adsorbed phase ( $m_{ads}$ ) can then be determined using Equation 6:

$$m_{ads} = M_{ads} n_{ads} = M_{He} HP \quad (6)$$

where  $H$  is the Henry constant for the adsorption isotherm, and  $M_{ads}$  is the molar mass of the adsorbed phase, which in this case is that of helium,  $M_{He}$ . By replacing  $P$  in Equation 6 with the ideal gas law ( $P = RT\rho_g$ ), Equation 5 can be expressed as follow:

$$m_{bal} = m_b + m_s + [M_{He} HRT - (V_b + m_s v_s)] \rho_g \quad (7)$$

The Henry's Law constant is a function of temperature, which can be expressed in the form of an Arrhenius-type equation<sup>1, 18</sup>:

$$H = H_0 \exp\left(\frac{H_I}{RT}\right) \quad (8)$$

where  $H_I$  is the helium isosteric heat of adsorption and  $H_0$  is related to the entropy of adsorption in the Henry's Law region<sup>2</sup>. Substituting Eq (8) into Eq (7) leads to the following empirical working equation, which can be regressed to gravimetric sorption data measured over a wide

range of temperature and pressure to determine optimised values for the three adjustable parameters of  $H_0$ ,  $H_1$ , and  $v_s$ .

$$m_{bal} = m_b + m_s + \left[ M_{He} H_0 \exp\left(\frac{H_1}{RT}\right) RT - (V_b + m_s v_s) \right] \rho_g \quad (9)$$

Implicit to the method is an assumption that the adjustable parameter,  $v_s$ , characterising the specific volume of the sample is independent of temperature over the range of the measured data. This assumption is reasonable for clinoptilolite: Bish et al.<sup>19</sup> used powder X-ray diffraction to analyse changes in the unit cell of several natural clinoptilolite samples and found a negative volumetric coefficient of thermal expansion on the order of  $10^{-9} \text{ K}^{-1}$ . Accordingly, in this work the natural clinoptilolite sample was assumed to have zero thermal expansion. The validity of this assumption may be tested further by observing the linearity of  $m_{bal}$  readings acquired as a function of gas density or pressure given the functional form of Eq (9), which was found to be the case for all of the helium adsorption isotherms shown below. For the analysis of the helium adsorption measurements made using the volumetric apparatus, the quantity  $V_s$  in Eq (2) was set equal to the value of  $v_s$  determined in the gravimetric measurements, multiplied by the sample mass loaded into the adsorption cell (44.151 g).

## 2.2 *Equilibrium adsorption measurements of pure nitrogen*

High-pressure adsorption isotherms of pure  $\text{N}_2$  on Escott zeolite were also measured at (303, 313 and 323) K and pressures up to 4.49 MPa using a BELSORP-BG instrument (BEL Japan) equipped with a RUBOTHERM magnetic floating balance. Before adsorption measurements, the adsorbents were degassed in-situ at 473 K for 24 hrs. We have described the operation of this apparatus elsewhere<sup>10</sup>.

## 3 **Results and Discussion**

Figure 3 shows the value of  $v_s$  determined from the gravimetric measurements with helium, while Figure 4 shows the corresponding helium adsorption equilibrium capacities determined from 253.15 K to 423.15 K at pressures to 35 MPa. The measured capacity data are also listed in Table 1S of the supplementary information (SI). The values of the best-fit parameters  $v_s$ ,  $H_0$  and  $H_1$  determined by regression of Eq (9) to these data are listed together with their statistical uncertainties in Table 1. The results of the helium adsorption measurements made using the volumetric apparatus are shown in Figure 5 and tabulated in Table 2S of the SI. Below we discuss the results of the helium adsorption measurements on the Escott zeolite made with the two apparatus in this work, and those determined previously using the Belsorp apparatus.<sup>10</sup> The

N<sub>2</sub> adsorption equilibrium capacities measured with the Belsorp apparatus are shown in **Figure 6** and listed in Table 4S of the SI. Finally, these results are used to speculate on the conditions at which the Escott zeolite might have a sufficiently favourable selectivity for He over N<sub>2</sub> for use in an adsorption process designed to recover helium from the overhead stream of an NRU in an LNG plant.

### **3.1 Impact of assuming negligible helium adsorption on the apparent specific solid volume**

Figure 3 **Error! Reference source not found.** shows the temperature independent value of  $v_s$  determined from regression of Eq (9) to the gravimetric sorption data together with apparent specific solid volumes ( $v_s^{(app)}$ ) calculated with the standard (incorrect) assumption of  $n_{ads} = 0$  in Eq (1) to (3) for the volumetric apparatus data and in Eq (5) for the data obtained with gravimetric apparatus. As observed previously<sup>10</sup>,  $v_s^{(app)}$  increases from the lowest to the highest experimental temperature. The agreement in the values of  $v_s^{(app)}$  obtained across three different apparatus is remarkable and within the combined experimental uncertainties of the data. The smaller  $v_s^{(app)}$  values obtained the lowest temperatures of 183 and 123 K reflect the greater uptake of helium at lower temperatures<sup>2-3, 20</sup>, although the experimental uncertainty of the measurements also increases as the signal-to-noise ratio of the volumetric measurements decreases and the uncertainty  $V_A(T)$  increases. The slightly larger values of  $v_s^{(app)}$  determined

using the gravimetric Belsorp apparatus described in reference 10 are attributable to the smaller pressure range (< 3.5 MPa) considered in those measurements.

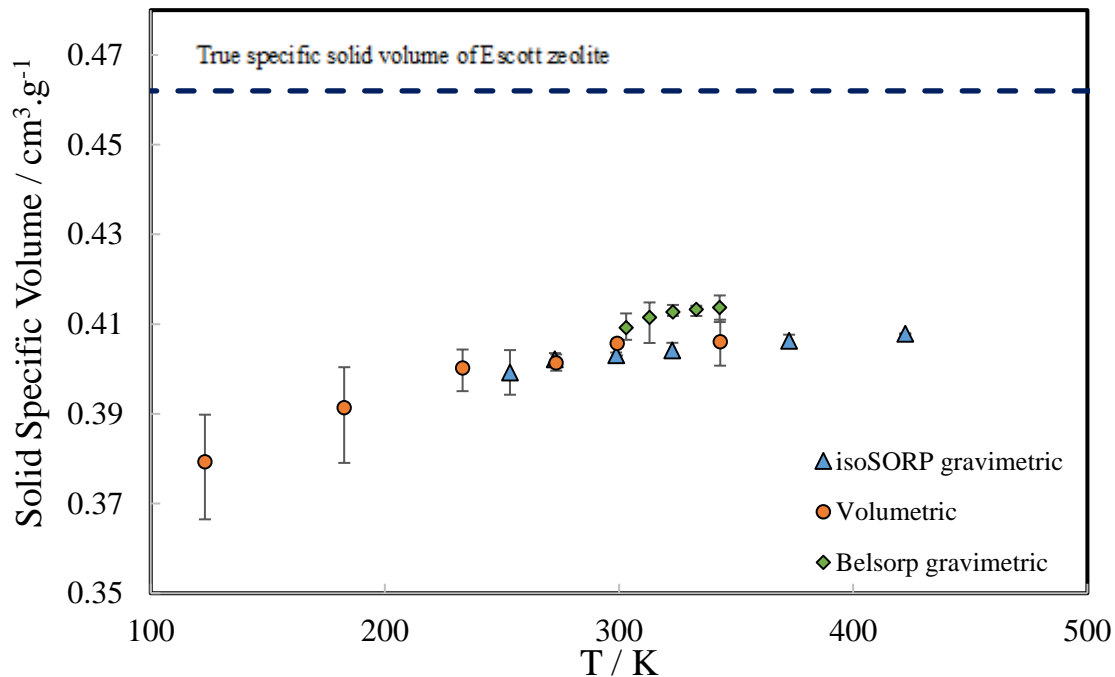


**Figure 3** Actual (dashed curve) and apparent (symbols) specific solid volume  $v_s$  of Escott zeolite determined from independent measurements completed using three instruments: (i) volumetric apparatus, (ii) isoSORP gravimetric apparatus, and (iii) Belsorp gravimetric apparatus.<sup>10</sup> The actual  $v_s$  is derived from the isoSORP measurements conducted in this work from (253 to 423) K at pressures to 35 MPa using Eq (9) and is consistent with XRD measurements of negligible expansivity.<sup>19</sup> The values of  $v_s^{(app)}$  were calculated by assuming  $n_{ads} = 0$  in Eq (1) to (3) for the volumetric data & in Eq (5) for the gravimetric data.

Similar trends in  $v_s^{(app)}$  with temperature were reported by Gumma and Talu<sup>2</sup> in the determination of Gibbs dividing surface of silicalite using helium. However, the variation in  $v_s^{(app)}$  with temperature would correspond to a volume thermal expansivity of  $3 \times 10^{-4} \text{ K}^{-1}$ , which is several orders of magnitude larger than that measured by XRD<sup>19</sup>. The results presented in Figure 3Error! Reference source not found., indicate that the anomalous dependence of the zeolite' specific volume on temperature is in fact a consequence of non-negligible helium adsorption<sup>5-6, 8</sup>.

### 3.2 Helium uptake on Escott Zeolite from gravimetric adsorption measurements

The best-fit parameters  $v_s$ ,  $H_0$ , and  $H_1$  of the model shown in Eq (9) were obtained using a least-

squares regression analysis of the equilibrium capacity data measured with the gravimetric isoSORP apparatus by minimizing the root mean deviation  $SD = ((1/N)\Sigma(m_{bal}^{Calc} - m_{bal}^{Meas})^2)^{1/2}$ .

Here  $N$  is the number of data points,  $m_{bal}^{Meas}$  is the measured mass and  $m_{bal}^{Calc}$  is the mass calculated with Eq 9. The best-values for the fitting parameters reported in Table 1 are consistent with but more accurate than those reported previously<sup>10</sup> given the wider range of experimental temperatures and pressures and the improved resolution of the measurement apparatus used in this work. The standard deviation of the fit was 2.59  $\mu\text{g}$  for the data measured in this work, which is about 10 times smaller than that achieved previously.

The value of  $H_I$  listed in Table 1 is comparable with the helium heats of adsorption for different adsorbents reported in the literature (Table 2). It's small magnitude is less than half that measured for  $\text{N}_2$  on Escott zeolite (Table 3), reflecting helium's absence of any permanent dipole or quadrupole moment and very weak adsorbate-solid interactions.

The helium equilibrium adsorption capacities for the clinoptilolite sample are shown in **Figure 4**. These were calculated from the measured values of  $m_{bal}$  by re-arranging Eq (5) to solve for  $m_{ads}$  using the  $v_s$  determined from the regression, and by then accounting for mass of the sample and helium's molar mass. The results are in good agreement with the previous measurement of helium adsorption on the clinoptilolite<sup>10</sup> at pressures below 3.5 MPa. The greatest adsorption of helium observed was 0.9 mmol.g<sup>-1</sup> at 253 K and 35 MPa. The extent of helium adsorption expected based on the Henry's Law parameters  $H_0$  and  $H_I$  listed in Table 1 is also shown for the highest and the lowest temperatures in **Error! Reference source not found.**

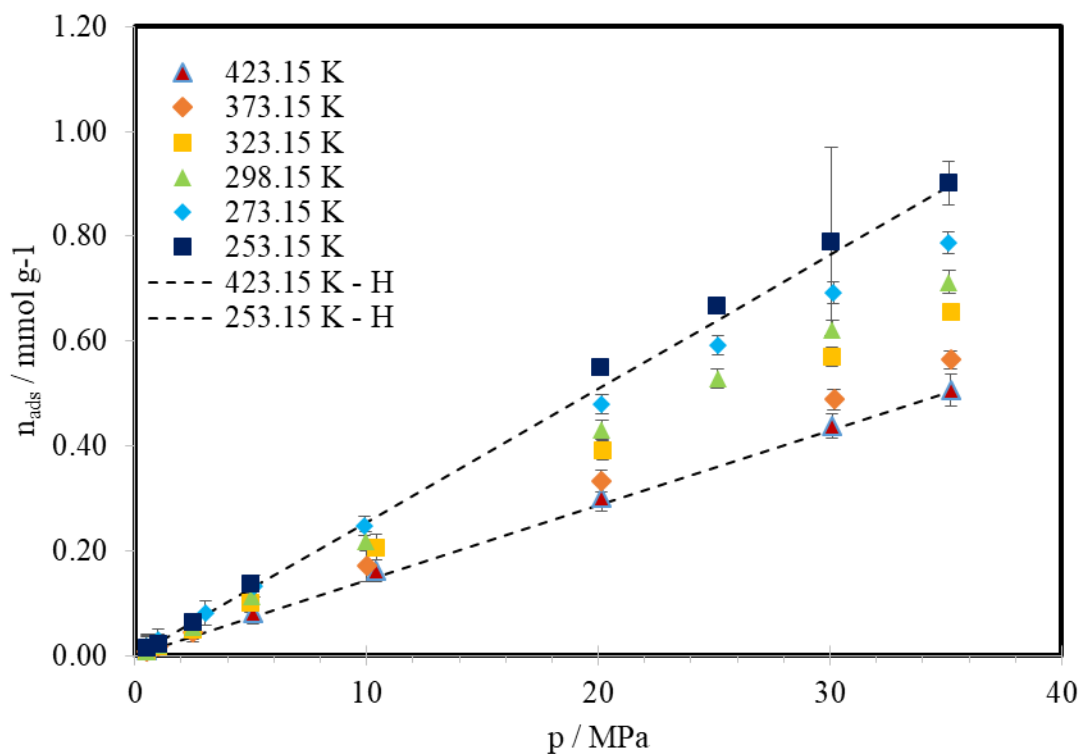


**Figure 4** Helium surface excess adsorbed amount on clinoptilolite derived from the  $m_{bal}$  readings acquired with the isoSORP gravimetric apparatus at temperatures from 253.15 K to 423.15 K. The error bars marked on the 303.15 K isotherm represent the uncertainty in the helium adsorption capacity estimated from (1) the measurement uncertainty in the magnetic suspension balance and (2) the uncertainties that result from the data analysis procedures used to determine  $v_s$ . The dashed lines show the Henry's Law behaviour expected from the regressed values of  $H_0$  and  $H_1$ .



**Table 1** Apparent specific solid volume for Escott Zeolite determined from three independent measurements, together with best-fit values obtained by fitting parameters in Eq (9) to the gravimetric sorption capacity data and the standard deviation between the measured and calculated mass data. The pycnometer value is based on the assumption that no helium is adsorbed by the sample under study.

	Temperature range (K)	Maximum pressure (MPa)	$v_s$ ( $\text{cm}^3 \cdot \text{g}^{-1}$ )	$10^3 H_0$ ( $\text{mmol} \cdot (\text{kg} \cdot \text{kPa})^{-1}$ )	$H_I$ ( $\text{kJ} \cdot \text{mol}^{-1}$ )	SD ( $\mu\text{g}$ )
<b>Conventional Helium pycnometer</b>	298.15	0 – 0.1013	0.422	-	-	-
<b>Belsorp gravimetric<sup>10</sup></b>	303.15 – 343.15	3.5	0.461	5.14	3	39
<b>isoSORP gravimetric</b>	253.15 – 423.15	35	$0.4618 \pm 0.0001$	$(6.000 \pm 0.001)$	$3.05 \pm 0.35$	2.56

**Table 2** The helium heat of adsorption values on different adsorbents reported in literature.

Adsorbent	$H_1$ (kJ.mol <sup>-1</sup> )	Reference
5A Zeolite	5.82	
13X Zeolite	4.64	
SXC Carbon (1670 m <sup>2</sup> .g <sup>-1</sup> ).	4.94	1
BPL Carbon (1120 m <sup>2</sup> .g <sup>-1</sup> ).	3.1	
Alumina (113 m <sup>2</sup> .g <sup>-1</sup> )	2.92	
Silicalite	3.9	2
Cylindrical carbon nanopores	3.58	21
Zeolite NaA	1.95	22
Natural Clinoptilolite (Escott zeolite)	3.16	This work

### 3.3 Helium uptake on Escott zeolite using volumetric adsorption apparatus

Using the  $v_s$  value determined from the gravimetric measurements, the amount of surface excess adsorbed helium on the natural clinoptilolite determined with the volumetric apparatus were calculated over the temperature range of (123 to 343) K using Eqs 1 to 3. Figure 5 shows the resulting helium adsorption equilibrium capacities as a function of pressure, which have a linear trend up to the maximum pressure measured (5 MPa). The volumetric data have relatively large estimated uncertainties, as shown by the error bars on the 123 K isotherm, which are mainly due to the measurement's limited signal to noise caused by (1) the small quantity of helium adsorption, and (2) the large values of  $V_A$  and  $V_L$ . Other contributions to the measurement uncertainty include the volume calibration, and the long-term performance of the temperature sensors at cryogenic conditions.

Figure 5 also shows adsorption isotherms predicted using the Henry's law parameters determined by regression to the gravimetric data measured at higher temperatures. In general the predicted isotherms are reasonably consistent with the measured uptake, particularly considering the extent of the extrapolation. At the lowest temperature of 123 K, the predicted adsorption capacity isotherm is higher than the measured uptake by more than the experimental uncertainty. However, the prediction and measurements agree within the combined uncertainty of the model and the data; if the value of  $H_1$  used is reduced by its statistical uncertainty from

3.05 to 2.7 kJ.mol<sup>-1</sup>, the prediction adsorption capacities agree with all the values measured at 123 K within the estimated experimental uncertainty.

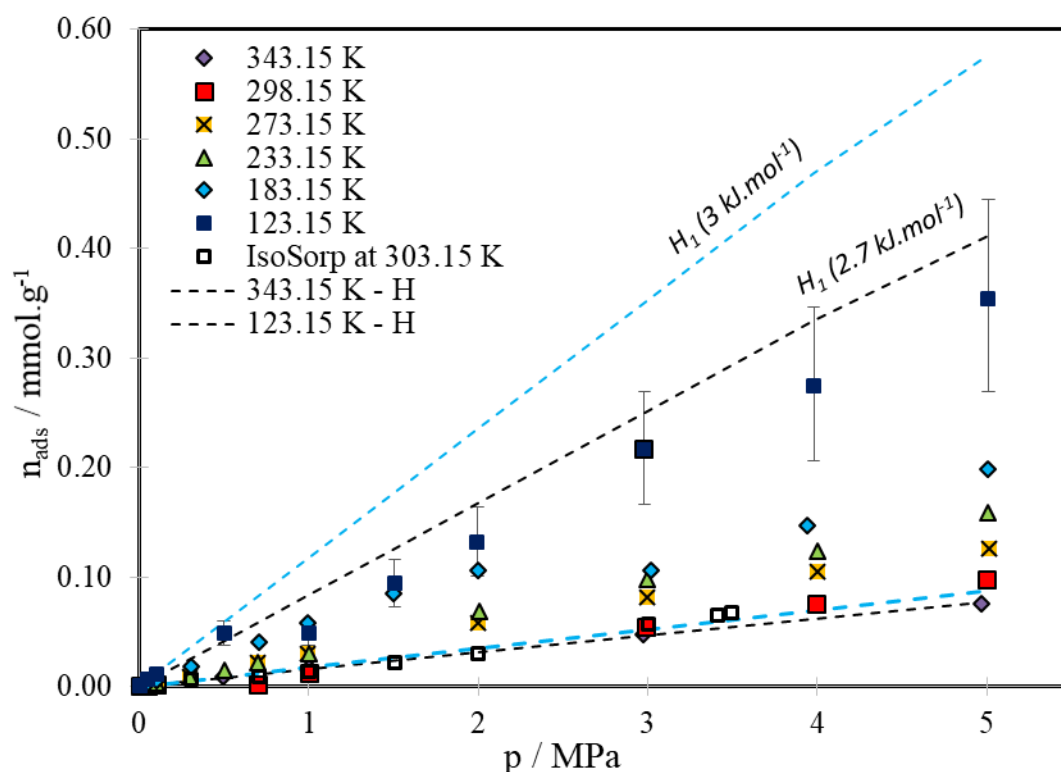


**Figure 5** Helium surface excess adsorbed amount on clinoptilolite in the temperature range of (123.15 to 343.15) K using the volumetric apparatus with a temperature independent  $v_s$  as determined from the gravimetric measurements made using the isoSORP apparatus. The dashed lines show the Henry's Law behaviour predicted using the values of  $H_0$  and  $H_1$  determined from the gravimetric sorption data and extrapolated to lower temperatures. the lower range value of  $H_1$  (2.7 kJ.mol<sup>-1</sup>) shows better consistency with the adsorption data.

These measurements reveal that although small, helium adsorption on this small pore zeolite at ambient temperature and moderate pressures is small but non-zero. This has implications for the determination of the adsorption of other gases when a helium calibration is used to determine the sample's volume under the assumption  $n_{\text{ads}} = 0$ . For example for the uptake of CO<sub>2</sub> at 3.5 MPa and 303.15 K, which was measured previously by Arami-Niya et al.<sup>10</sup>, conventionally helium pycnometry of the Escott zeolite leads to a measured adsorption capacity of 0.9 mmol.g<sup>-1</sup>. In contrast, accounting for the adsorption of helium even at these moderate conditions leads to an adsorption capacity of 0.97 mmol.g<sup>-1</sup> for CO<sub>2</sub> at this condition. It is apparent that the error is about the same as the magnitude of helium adsorption at the temperature and pressure of interest.

### 3.4 He / N<sub>2</sub> Selectivity of Escott zeolite

One possible application of the Escott zeolite is the selective adsorption of helium from an NRU vent stream. To quickly assess the viability of an adsorption-based process for helium recovery, the N<sub>2</sub> adsorption capacity of the Escott zeolite was also measured over a limited range. The excess adsorption capacities of N<sub>2</sub> on Escott zeolite measured with the gravimetric BELSORP-BG apparatus at temperatures of (303, 313 and 323) K are shown in Figure 6 with tabulated adsorption equilibria provided in **Error! Reference source not found.S**. As expected, the narrow pores of the Escott zeolite limit the uptake of N<sub>2</sub> molecules, although at 5 MPa the N<sub>2</sub> adsorption capacity of around 0.25 mmol.g<sup>-1</sup> is about twice that of helium at the same conditions. We note that if a value of  $v_s$  determined by calibration with helium under the assumption of  $n_{\text{ads}} = 0$  were used to analyse the N<sub>2</sub> uptake, the capacity would be underestimated by about 0.1 mmol.g<sup>-1</sup> at 5 MPa (Figure 1S).

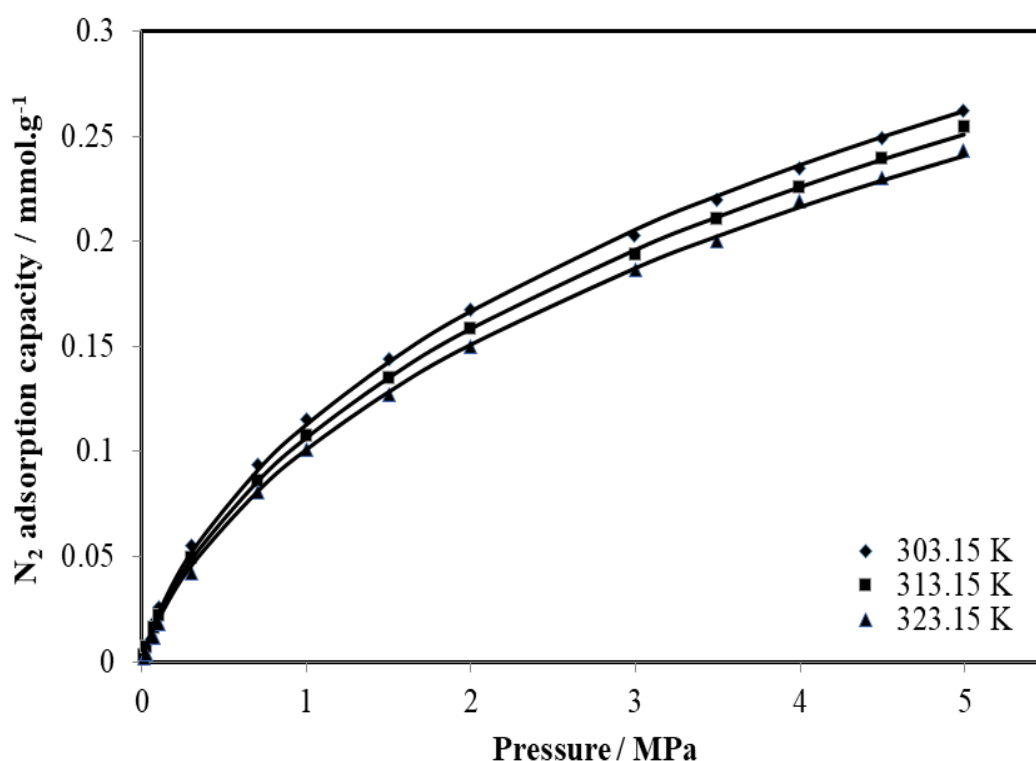


**Figure 6** Uptake of N<sub>2</sub> on the clinoptilolite (Escott zeolite) measured at temperatures of 303.15 K, 313.15 K and 323.15 K and pressures up to 5 MPa. The solid lines show the resulting Toth model regressed to the data.

The measured N<sub>2</sub> data were fit to the temperature-dependent Toth model:

$$Q = Q_m \frac{BP}{[1 + (BP)^t]^{1/t}} \quad \text{where } B = B_0 \exp\left(\frac{-\Delta H}{RT}\right) \quad (10)$$

where  $R$  is the molar gas constant,  $P$  and  $T$  are the measurement pressure and temperature, and  $\Delta H$  is the isosteric heat of adsorption at zero loading. In the regression  $\Delta H$  was treated as an adjustable parameter together with the empirical parameters ( $Q_m$ ,  $B_0$ ,  $t$ ). The parameter  $t$  is used to characterize the heterogeneity of the adsorption sites and should have a value less than 1. The best fit parameters were determined using a least-squares regression analysis to minimize the standard deviation (SD) between the measured capacities,  $Q^{meas}$ , and the capacities  $Q^{calc}$  calculated with each model ( $SD = ((1/N)\Sigma(Q^{meas} - Q^{calc})^2)^{1/2}$  where  $N$  is the number of data points regressed). The best-fit parameters for the Toth model regressed to the N<sub>2</sub> data are shown in **Table 3**, together with their statistical uncertainties. Deviations between the measured and the calculated adsorption capacities for pure N<sub>2</sub> are shown in Figure 2S.

**Table 3** Best fit parameters of the Toth Model (**Error! Reference source not found.**) fitted to the absolute adsorption capacities for N<sub>2</sub> on Escott zeolite measured on the Belsorp-BG at 303 K, 313 K, and 323 K.

	N <sub>2</sub>
$Q_m$ (mmol. g <sup>-1</sup> )	1.43 ± 0.28
$b_0 \times 10^6$ (kPa <sup>-1</sup> )	17.4 ± 2.5
$\Delta H$ (J.mmol <sup>-1</sup> )	7.50 ± 0.45
$t$	0.35 ± 0.03
$SD$ (mmol.g <sup>-1</sup> )	0.002

The equilibrium selectivity,  $\alpha_{ij}$ , is defined as:

$$\alpha_{ij} = \left(\frac{x_i}{x_j}\right)\left(\frac{y_j}{y_i}\right) \rightarrow \alpha_{ij} = \left(\frac{Q_i}{Q_j}\right)\left(\frac{y_j}{y_i}\right) \quad (11)$$

where  $y$  and  $x$  are the mole fraction of component  $i$  and  $j$  in the vapor and adsorbed phases, respectively. The values of  $Q_i$  were calculated for a gas mixture of varying composition using the Ideal Adsorbed Solution Theory<sup>23</sup> together with the pure fluid adsorption isotherms

determined in this work. For helium, the isotherm function was  $n_{ads}=HP$ , with  $H$  calculated from Eq (8) using the parameters in Table 1, while for  $N_2$  the isotherm function was Eq (10) using the parameters listed in Table 3. Figure 7(a) shows calculated equilibrium selectivities of the natural clinoptilolite (Escott) for He over  $N_2$  as a function of gas mixture composition (at fixed temperature and pressure). Figure 7(b) shows calculated selectivities as a function of temperature for an equimolar gas mixture at fixed pressures.

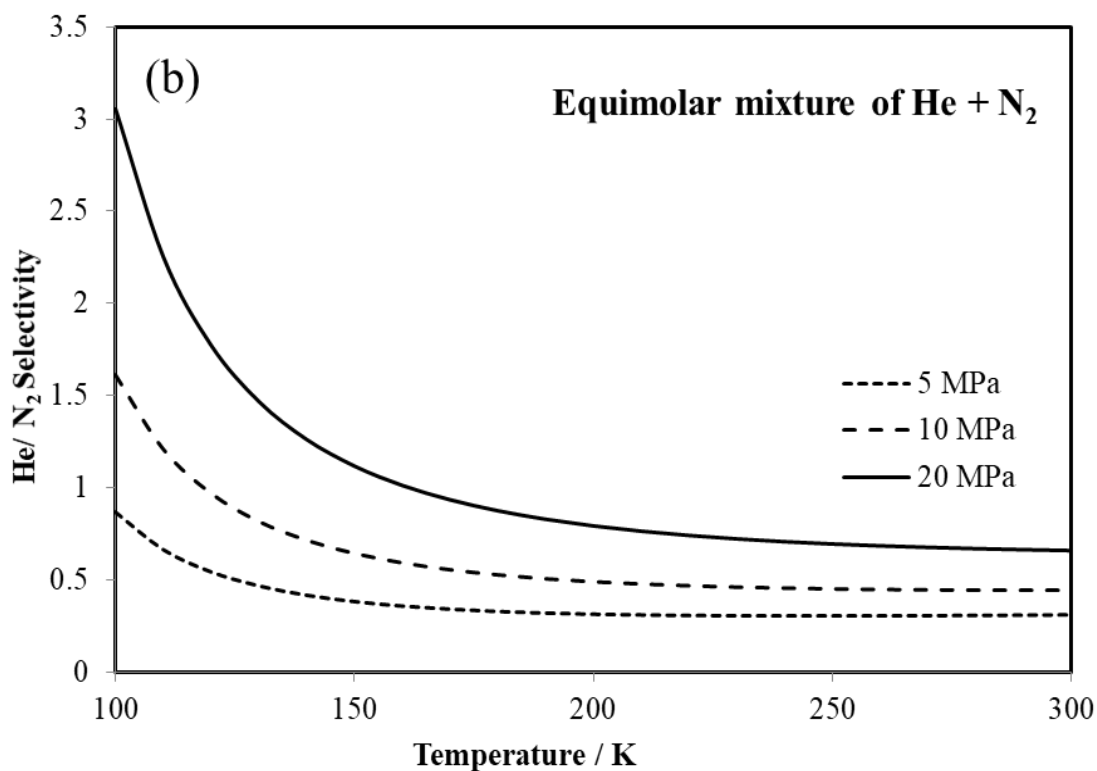
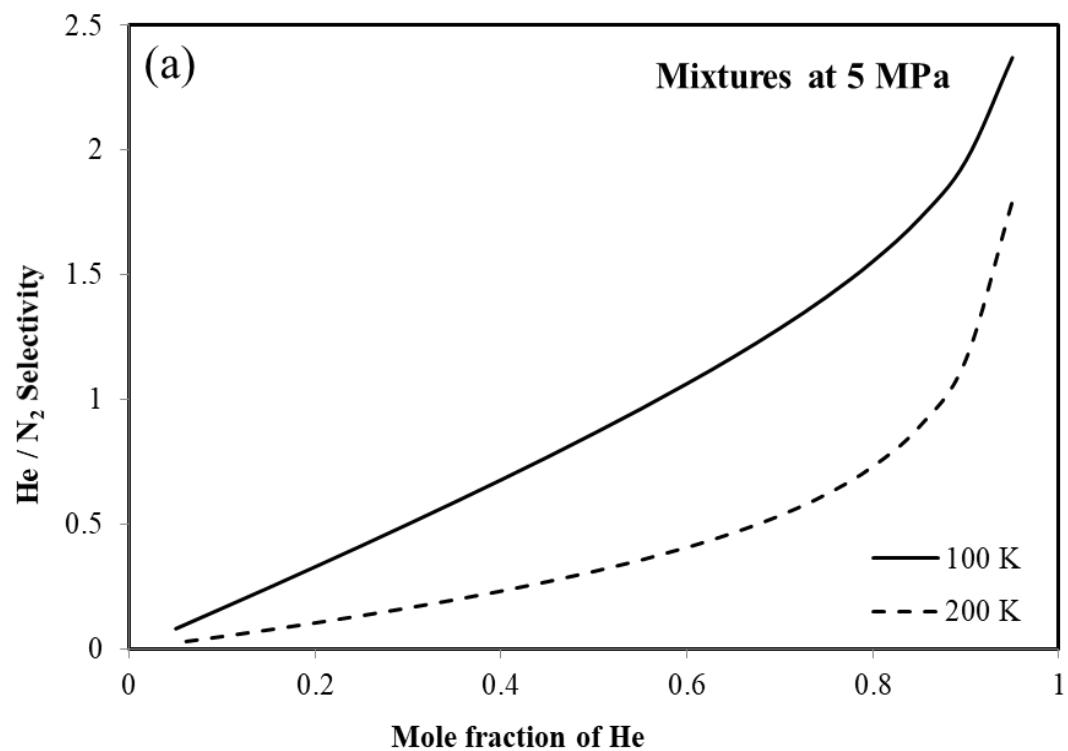


**Figure 7** He/N<sub>2</sub> equilibrium selectivities of the Escott zeolite, predicted using the IAST with the pure fluid isotherms determined in this work as a function of (a) gas mixture composition (fixed temperature and pressure) and (b) temperature at fixed pressure for an equimolar mixture.

Decreasing the temperature or increasing the (partial) pressure of the helium all act to increase the calculated He / N<sub>2</sub> equilibrium selectivity of the Escott zeolite. For an equimolar mixture, the He / N<sub>2</sub> equilibrium selectivity is predicted to reach about 3 at 20 MPa and 100 K. Potentially, the effective selectivity for helium could be significantly higher than this value if the effect of adsorption kinetics is considered. The typical framework structure of clinoptilolite is formed by three sets of intersecting channels, A, B and C, based on eight and ten member rings, with approximate dimensions of 4.4×7.2 Å, 4.1×4.7 Å and 4.0×5.5 Å<sup>24</sup>. The locations of the framework cations within these channels lead to effective pore sizes that restrict the diffusion of relatively larger gas molecules such as N<sub>2</sub> (kinetic diameter of 3.64 Å). The kinetic diameter of smaller gas molecules such as H<sub>2</sub> and He (with about 2.89 and 2.60 Å, respectively)<sup>25</sup> means that they can diffuse into the clinoptilolite much faster than N<sub>2</sub>. The relative differences in diffusivity between He and N<sub>2</sub> in these narrow micropores will also be affected significantly by the process temperature, as diffusion becomes even slower at lower temperatures for larger molecules<sup>26-27</sup>.”

#### 4 Conclusions

In this work, we estimated the adsorbent's volume in high pressure gravimetric and volumetric adsorption measurement apparatus using two different assumptions of 1- negligible helium adsorption at the highest experimental temperature, and 2- helium is an adsorbing gas at all the temperatures. The true density of natural clinoptilolite (Escott zeolite) and its helium adsorption capacity was measured over a wide temperature range of 123.15 – 423.15 K and at pressures up to 35 MPa. The adsorbent's apparent specific volume as measured by conventional helium pycnometry in both gravimetric and volumetric systems increased with temperature. In contrast, using the method developed by Gumma and Talu<sup>2</sup>, the helium adsorption data obtained with the gravimetric system were used to determine the adsorbent's true specific volume. The helium sorption data were fit to a Henry's Law model to estimate the heat of adsorption as a function of temperature. The adsorbent's true specific volume was used to determine helium sorption at temperatures below 253 K using a volumetric apparatus. We always observed linear helium adsorption isotherms consistent with Henry's Law. The highest adsorption of helium observed across all these measurements was 0.9 mmol.g<sup>-1</sup> at 253 K and 35 MPa.

The adsorption capacity of N<sub>2</sub> on Escott zeolite was also measured and then used to calculate the IAST equilibrium selectivity of He over N<sub>2</sub> for a range of compositions, from 5 to 20 MPa



and from 100-300 K. Helium selectivity increases at low temperatures and high pressures achieving a value as high as 3 for an equimolar mixture at 100 K and 20 MPa. However, at 5 MPa the Escott zeolite is N<sub>2</sub> selective in equimolar mixtures over the temperature range considered. These results help inform whether and how Escott zeolite could be used in the design of adsorption based technologies for the production of helium; the measurement techniques described can be applied to other microporous materials for similar purposes.

## Acknowledgments

This research received funding from the Australian Research Council through the ARC Training Centre for LNG Futures (<http://lngfutures.edu.au/>, IC150100019).

## References

1. Sircar, S., Measurement of gibbsian surface excess. *AIChE Journal* **2001**, *47* (5), 1169-1176.
2. Gumma, S.; Talu, O., Gibbs Dividing Surface and Helium Adsorption. *Adsorption* **2003**, *9* (1), 17-28.
3. Malbrunot, P.; Vidal, D.; Vermesse, J.; Chahine, R.; Bose, T. K., Adsorbent Helium Density Measurement and Its Effect on Adsorption Isotherms at High Pressure. *Langmuir* **1997**, *13* (3), 539-544.
4. Lachawiec, A. J.; DiRaimondo, T. R.; Yang, R. T., A robust volumetric apparatus and method for measuring high pressure hydrogen storage properties of nanostructured materials. *Review of Scientific Instruments* **2008**, *79* (6), 063906.
5. Lorenz, K.; Wessling, M., How to determine the correct sample volume by gravimetric sorption measurements. *Adsorption* **2013**, *19* (6), 1117-1125.
6. Maggs, F. A. P.; Schwabe, P. H.; Williams, J. H., Adsorption of Helium on Carbons: Influence on Measurement of Density. *Nature* **1960**, *186* (4729), 956-958.
7. Talu, O.; Myers, A. L., Molecular simulation of adsorption: Gibbs dividing surface and comparison with experiment. *AIChE Journal* **2001**, *47* (5), 1160-1168.
8. Suzuki, I.; Kakimoto, K.; Oki, S., Volumetric determination of adsorption of helium over some zeolites with a temperature-compensated, differential tensimeter having symmetrical design. *Review of Scientific Instruments* **1987**, *58* (7), 1226-1230.
9. Huong Giang, T. N.; Jarod, C. H.; Matthias, T.; Roger, D. v. Z.; Laura, E., Experimental aspects of buoyancy correction in measuring reliable high-pressure excess adsorption

isotherms using the gravimetric method. *Measurement Science and Technology* **2017**, 28 (12), 125802.

10. Arami-Niya, A.; Rufford, T. E.; Birkett, G.; Zhu, Z., Gravimetric adsorption measurements of helium on natural clinoptilolite and synthetic molecular sieves at pressures up to 3500 kPa. *Microporous and Mesoporous Materials* **2017**, 244, 218-225.

11. Chemical and Physical Analysis of Escott Zeolite. Zeolite Australia Pty Ltd: 2012.

12. Watson, G.; May, E. F.; Graham, B. F.; Trebble, M. A.; Trengove, R. D.; Chan, K. I., Equilibrium Adsorption Measurements of Pure Nitrogen, Carbon Dioxide, and Methane on a Carbon Molecular Sieve at Cryogenic Temperatures and High Pressures†. *Journal of Chemical & Engineering Data* **2009**, 54 (9), 2701-2707.

13. Rufford, T. E.; Watson, G. C. Y.; Saleman, T. L.; Hofman, P. S.; Jensen, N. K.; May, E. F., Adsorption Equilibria and Kinetics of Methane + Nitrogen Mixtures on the Activated Carbon Norit RB3. *Industrial & Engineering Chemistry Research* **2013**, 52 (39), 14270-14281.

14. Watson, G. C.; Jensen, N. K.; Rufford, T. E.; Chan, K. I.; May, E. F., Volumetric Adsorption Measurements of N<sub>2</sub>, CO<sub>2</sub>, CH<sub>4</sub>, and a CO<sub>2</sub> + CH<sub>4</sub> Mixture on a Natural Chabazite from (5 to 3000) kPa. *Journal of Chemical & Engineering Data* **2012**, 57 (1), 93-101.

15. Tegeler, C.; Span, R.; Wagner, W., A new equation of state for argon covering the fluid region for temperatures from the melting line to 700 K at pressures up to 1000 MPa. *Journal of Physical and Chemical Reference Data* **1999**, 28 (3), 779-827.

16. Lemmon, E. W.; Huber, M. L.; McLinden, M. O. *NIST Standard Reference Database 23: Reference Fluid Thermodynamic and Transport Properties (REFPROP), Version 9.1*, Gaithersburg, MD, USA, 2013.

17. Karimi, A.; Hughes, T. J.; Richter, M.; May, E. F., Density Measurements of Methane + Propane Mixtures at Temperatures between (256 and 422) K and Pressures from (24 to 35) MPa. *Journal of Chemical & Engineering Data* **2016**, 61 (8), 2782-2790.

18. Sircar, S., Gibbsian Surface Excess for Gas Adsorption Revisited. *Industrial & Engineering Chemistry Research* **1999**, 38 (10), 3670-3682.

19. Tschauferer, P.; Parker, S. C., Thermal Expansion Behavior of Zeolites and AlPO<sub>4</sub>s. *The Journal of Physical Chemistry* **1995**, 99 (26), 10609-10615.

20. Myers, A.; Monson, P., Physical adsorption of gases: the case for absolute adsorption as the basis for thermodynamic analysis. *Adsorption* **2014**, 20 (4), 591-622.

21. Liu, J.; LeVan, M. D., Isothermic heats of adsorption in the Henry's law region for carbon single wall cylindrical nanopores and spherical nanocavities. *Carbon* **2009**, 47 (15), 3415-3423.

22. Vashchenko, L. A.; Katal'nikova, V. V., Adsorption of helium on zeolite NaA. *Russian Chemical Bulletin* **1996**, 45 (5), 1230-1231.

23. Myers, A. L.; Prausnitz, J. M., Thermodynamics of mixed-gas adsorption. *AIChE Journal* **1965**, 11 (1), 121-127.

24. Ackley, M. W.; Yang, R. T., Adsorption characteristics of high-exchange clinoptilolites. *Industrial & Engineering Chemistry Research* **1991**, 30 (12), 2523-2530.

25. Aguilar-Armenta, G.; Hernandez-Ramirez, G.; Flores-Loyola, E.; Ugarte-Castaneda, A.; Silva-Gonzalez, R.; Tabares-Munoz, C.; Jimenez-Lopez, A.; Rodriguez-Castellon, E.,

Adsorption Kinetics of CO<sub>2</sub>, O<sub>2</sub>, N<sub>2</sub>, and CH<sub>4</sub> in Cation-Exchanged Clinoptilolite. *The Journal of Physical Chemistry B* **2001**, *105* (7), 1313-1319.

26. Barrer, R. M., FORMAL THEORY OF DIFFUSION THROUGH MEMBRANES. **1974**, 113-124.

27. Bhatia, S. K.; Bonilla, M. R.; Nicholson, D., Molecular transport in nanopores: a theoretical perspective. *Physical Chemistry Chemical Physics* **2011**, *13* (34), 15350-15383.